ORIGINAL PAPER

Thermal Energy Storage Material Based on High Density Polyethylene Filled with Graphene Oxide Modified Microencapsulated Eutectic Mixture of Fatty Acid

Shriya J. Jaiswal[1] · Shrutika N. Sonare[1] · Prakash A. Mahanwar[1]

Abstract

To store thermal energy, a composite material was created using high density polyethylene (HDPE) filled with microencapsulated phase change material (PCM). The microcapsules consist of a eutectic mixture of myristic acid (MA) and stearic acid (SA) as the PCM core, which is encapsulated using in-situ polymerization of graphene oxide (GO) modified melamine formaldehyde (MF). The addition of GO was made to improve thermal conductivity. Both the microcapsules and composite material underwent different characterization and mechanical testing. Lee's method was used to examine microcapsules with a standard MF shell and those with a GO modified MF shell (g-MF) for thermal conductivity. The microcapsules with 0.8% GO shell had the highest % increase of 47.5% in thermal conductivity. The differential scanning calorimetry (DSC) results showed that the PCM had a melting point of 42 ˚C with a latent heat of 145 J/g and a crystallization point at 35˚C with a latent heat of 139 J/g. Characterization methods such as scanning electron microscopy (SEM) and polarized optical microscopy (POM) confirmed the formation of a core–shell structure with a smooth morphology. Thermogravimetric analysis (TGA) results indicated improved thermal stability of PCM due to encapsulation, and Fourier transform infrared spectroscopy (FTIR) showed negligible interaction between the core and shell material. A custom-made heat transfer rate equipment was used to study the heat transfer rate through the composite material. It indicated a lower heat transfer rate through the composite material than through virgin HDPE.

Keywords Eutectic mixture · Phase change material · Thermal conductivity · Thermoplastic composite · High density polyethylene (HDPE)

Introduction

Storing thermal energy presents a promising solution to the ongoing challenge of meeting rising energy demand. In comparison to other forms of energy storage, such as mechanical, electrical, and chemical, thermal energy storage (TES) has been shown to be particularly suitable [1]. Thermal energy can be stored in diverse ways, such as through thermochemical, latent heat, sensible heat, or a combination of these methods. Thermochemical energy storage devices store energy by breaking chemical bonds at the molecular level, releasing energy that can later be recovered through a reversible chemical reaction. Sensible heat storage (SHS), on the other hand, involves adding energy to raise the temperature of a material without changing its phase. The amount of heat that can be stored through SHS depends on a range of factors, such as the quantity of storing material, temperature changes, and the heat capacity of the substance. Solid storage materials, such as rocks, concrete, sand, and bricks, as well as liquid storage materials, such as water, mineral oil, molten salts, liquid metals, and alloys, can be used for SHS. Latent heat storage (LHS) refers to the heat that is released or absorbed when a storage substance changes from liquid to solid, liquid to gas, or vice versa. The storage material used for LHS is called phase change material (PCM). LHS offers a higher energy storage density with almost no change in temperature compared to SHS [1] [2] [3].

Distinct types of PCMs, such as salt hydrates, paraffin, and fatty acids, have been explored for their potential uses. However, fatty acids stand out due to their exceptional

✉ Shriya J. Jaiswal
  shriyajas97@gmail.com

1   Department of Polymer and Surface Engineering, Institute of Chemical Technology, Mumbai, Maharashtra, India

qualities, such as easy continuous availability, chemical stability, congruent melting, relatively high latent heat of fusion in small volumes, minor volume change, and other characteristics[4] [5]. Eutectic mixtures of fatty acids have been researched in several literatures to take advantage of their benefits over other listed PCMs. This has also increased the phase change temperature range, ultimately expanding the spectrum of applications for fatty acids as PCMs[5]. The proper composition of fatty acids is crucial for forming a eutectic mixture with a single melting point. This requires studying the phase diagram of the mixture to determine the eutectic temperature and composition [6]. Thermal parameters required for different eutectics as PCMs for LHS systems are studied in [7] [4]. The calculation of the mass ratio of components of binary eutectic mixtures by the Schrader equation is explained in [8] [9]. In [10], the author has validated same formula as Eq. 1 for 15 fatty acid binary eutectic mixtures and theoretically calculated their thermal properties.

$$T_m = \left[\frac{1}{T_a} - R \times \frac{\ln X_a}{\Delta H_{ma}} \right]^{-1} \qquad (1)$$

$$T_m = \left[\frac{1}{T_b} - R \times \frac{\ln X_b}{\Delta H_{mb}} \right]^{-1} \qquad (2)$$

To prevent PCM from leaking out of the substrate, it can be encapsulated in macro, micro, or nano-sized shells or stabilized in a particular shape using a porous material. Various substrates, such as expanded graphite[11], wood flour [12],expanded vermiculite[9], polymer [13], can be used for shape stabilization. For microencapsulation, the shell can be organic or inorganic, such as silica [14], polyamide [15], polymethylmethacrylate (PMMA) [16], melamine formaldehyde (MF) [17], among others. In [18] researcher, encapsulated 46.2 wt.% of lauric acid in MF shell and got heat of fusion equal to 84.96 J/g. In article [19], the authors investigated effect of process parameter of encapsulation of paraffin in carboxymethyl cellulose modified urea formaldehyde shell.

The thermal conductivity of organic microcapsule shell materials such as PMMA, polyester, and MF is low. This results in limitations in the heat absorption of the core PCM material, which ultimately reduces the efficiency of the storage system. However, research has shown that the inclusion of thermal conductive additives in PCM microcapsules can improve the thermal conductivity of the material. These additives are typically metallic or carbon-based. Metal-based additives, such as metal foams, have a significant impact on improving thermal conductivity. However, metals have some significant drawbacks, such as low chemical resistance and low heat resistance. Carbon-based additives, on the

other hand, use different types of graphite, such as expanded graphite (EG), graphene oxide (GO), graphene nanoplates (GNP), etc. [20] [21] [22]. In [23] microcapsules containing paraffin as the PCM and graphene modified MF shell were made, and the effect of different graphene concentrations and core to shell ratios were studied. Another study [24] was carried out with dodecanol as PCM, MF as shell, and GO as a modifier. In [25], super hydrophobic self-cleaning microcapsules containing stearic acid and graphene oxide modifications were discussed. In [26], a comparison of GO and carbon nanotube (CNT) additions for improving thermal conductivity in microcapsules with a dodecanol core and MF shell was conducted. Finally, the authors of [27] used the Pickering suspension polymerization technique to create polyurea microcapsules containing n-eicosane and using GO as a colloidal stabilizer and thermal conductivity booster.

The application of PCM microcapsules is widespread in various fields where thermal energy storage, heat transfer, and temperature control are required. MEPCM can be incorporated into textiles using different methods, such as coating, lamination, and spinning, to produce thermoregulated clothing [28] [29] [30] [31]. Additionally, MEPCM can be added to building materials such as concrete and flooring by physically mixing it with other ingredients. In [32] a successful 4 months experiment with MEPCM slurry in a cold ceiling system at Narita airport in Tokyo for cold energy storage and temperature maintenance is discussed. Similarly, MEPCM can be mixed with paints to make heat insulating coating, with foam in various insulation systems like vehicle interiors, cool storages boxes etc. [28] [33]. Other application involves blending it with polymer as filler or using polymer as substrate to make form stable PCM. In [34], twin screw extruder technology is used to create a paraffin and HDPE composite with three different additives, EG, ammonium polyphosphate, and zinc borate, and its utilization in halogen-free flame retardants is researched. In [35][35],two different methods of blending HDPE with microcapsules having paraffin as PCM and MF as the shell were compared for their thermal and mechanical behaviour.

In reference [37], a study was conducted on a floor cooling system consisting of a composite material made up of nano-encapsulated PCM, wood fibre, and HDPE. Similarly, reference [38], investigates a composite made of low density polyethylene (LDPE), EG, and paraffin for potential use in battery thermal management (BTM) technologies. In reference [39], the fabrication and analysis of polypropylene (PP) yarns containing paraffin-MF microcapsules (commercial MPCM43D) for use in multifunctional thermoplastic laminates is described. Several sources provide a wealth of information on the development of stable PCM and polyolefin composites, including references [40] [41] [42].

After conducting a thorough literature review, this study demonstrates a unique combination of materials and

methods that can expand the application of eutectic mixtures as phase change materials (PCMs). Specifically, the study focuses on the preparation of a GO-modified MEPCM-filled HDPE composite (GO-MEPCM-HDPE) that uses a eutectic mixture of stearic acid (SA) and myristic acid (MA) as the PCM and GO-modified MF as the shell, prepared through a high %solid method by in-situ polymerization process. However, organic compounds typically have low thermal conductivity, which can hinder the efficiency of thermal storage in the PCM. Many articles describe incorporating thermal conductivity enhancers in the PCM as additives or shape stabilizers. In this study, we made a successful attempt to add a thermal conductivity enhancer in the shell material by varying the concentration of GO based on the weight percent of theoretical cross-linked polymer to analyse the threshold concentration of GO. We produced this concentration of GO-containing microcapsules in bulk and mixed it with HDPE using a twin-screw extruder in different ratios to determine the highest possible loading of microcapsules in the composite with manageable processability. We then evaluated this material using Lee's method for thermal conductivity, analysed it with various characterization techniques, and examined its effect on mechanical properties. Finally, we made a small prototype box to confirm the success of the material, which can be used for storage boxes or solar walls.

Materials and Methods

Material

Formaldehyde solution (37–40% w/v) was bought from Molychem Chemicals, Mumbai; Acetic Acid (99.7% analytical grade), Melamine, Stearic Acid (SA) (98% extra pure), Myristic Acid (MA) (98% extra pure), and Polyvinyl Alcohol (PVA) were taken from Loba Chemie, Mumbai; Sodium Lauryl Sulphate (SLS) (extra pure), Sodium Hydroxide pellets (98% extra pure), were acquired from SD fine chemicals, India; Graphene Oxide (GO) Nano particle was received

from Adnano Technologies, Karnataka. High density Polyethylene was taken from IOCL.

Method

Eutectic Mixture, GO Dispersion Preparation

According to Schrader's equation, a eutectic mixture was made using 26.71 wt.% of SA and 73.14 wt.% of MA. The acids were melted separately, mixed together, and stirred for one hour at 80 °C and 800 rpm.

To prepare the graphene oxide solution, take 3 g of Graphene Oxide and add distilled water to obtain a concentration of 0.3%. Sonicate the solution for 20 min.

Microencapsulation Process

The SA-MA PCM microcapsule is created using an in-situ polymerization process. This section describes the formulation with a high solid content. Firstly, 40 g of a melted eutectic mixture is combined with 60 ml of a sodium lauryl sulphate (SLS) solution in a 4-neck reactor with a condenser and stirrer in a thermostat. The mixture is then stirred for 15 min at 70 ˚C. Next, acetic acid is used to adjust the pH of the emulsion to an acidic range of 3 to 4, and stirring continues for an additional 40 min.

Following this, 20 ml of a 1% PVA solution is added dropwise at a rate of 1 drop every 2 s, and the emulsion is stirred for another 20 min. Meanwhile, a MF prepolymer is prepared by combining 14 g of melamine, 39 g of 37% formaldehyde, and the necessary amount of GO in a beaker. The solution is stirred at 70˚C until it turns transparent brown. The volume of GO dispersion is adjusted to obtain the actual weight of GO between 0.2 and 1.2 wt.% theoretical weight of the cross-linked shell material (Table 1). The pH of the prepolymer is adjusted to 7–8 using 1N sodium hydroxide solution.

The prepolymer is then added dropwise to the reaction flask for 45 min and stirred for 2 h to allow the MF to

Table 1 Formulation with GO variation

Materials batch	PCM (g)	Water (ml)	SLS (g)	PVA (ml)	GO (0.3% concentration, ml)	Melamine (g)	Formaldehyde (37% concentration, g)
Plain	40	60	1.64	20	0	14	39
0.2 GO	40	60	1.64	20	12.9	14	39
0.4 GO	40	60	1.64	20	25.8	14	39
0.6 GO	40	60	1.64	20	38.7	14	39
0.8 GO	40	60	1.64	20	51.6	14	39
1 GO	40	60	1.64	20	64.5	14	39
1.2 GO	40	60	1.64	20	77.4	14	39

polymerize. After 2 h, the pH is adjusted to a basic level, and the microcapsules are centrifuged and dried at 75°C for 24 h, resulting in SA-MA microcapsule powder.

MEPCM/HDPE Composite Preparation

Dried microcapsule was mixed with HDPE in required amount (Table 2) and blended properly with the help of twin screw extruder at screw speed of 40 rpm and temperature range from feed to die of 170 °C to 215 °C. Then extruded strands were palletized and compression moulded to form sheets. These sheets are used to make a prototype box for experimental purpose. Keeping microcapsule loading constant at 20% in composite GO containing microcapsules were varied first to check effective GO loading. Then effective loading GO containing microcapsule were used for varying microcapsule loading in composite. (Fig. 1).

Characterization

Thermal Properties

To analyse the thermal properties of the SA-MA eutectic PCM, plain microcapsules, microcapsules with GO variants, and microcapsule filled HDPE, Differential Scanning Calorimetry (DSC) (DSC-TA Q100) was employed. The temperature cycle ranged from 0 °C to 50 °C with a 5 °C/min heating and cooling rate.

Chemical Composition

To analyse the chemical composition of SA-MA eutectic PCM, MF shell, plain microcapsules, and microcapsule containing GO, Fourier Transform Infrared Spectroscopy

Table 2 Composite Variation

GO%	Microcapsule (g)	HDPE (g)	Effective GO loading (0.8%)	HDPE (g)	Plain MEPCM (g)		Total (g)
0	47	188		195	20%	50	250
0.2	47	188		175	30%	75	250
0.4	47	188		150	40%	100	250
0.6	47	188		HDPE (g)	0.8% GO MEPCM (g)		Total (g)
0.8	47	188		195	20%	50	250
1	47	188		175	30%	75	250
1.2	47	188		150	40%	100	250

Fig. 1 Procedural Overview
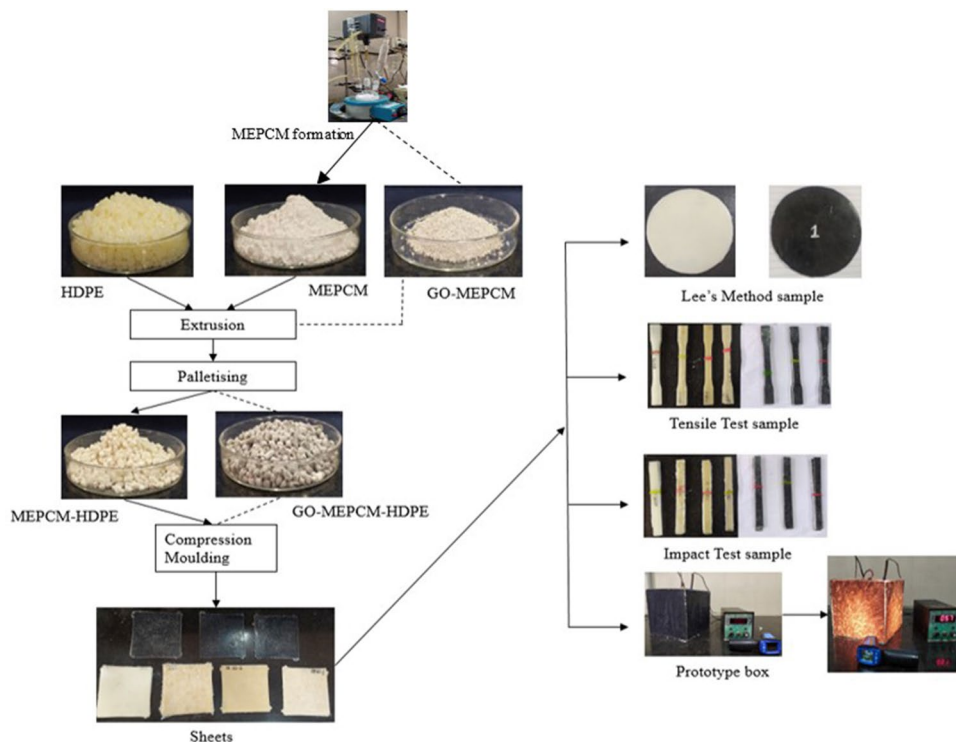
(FTIR) (FTIR-Bruker) using the Attenuated Total Reflectance (ATR) method was used. Furthermore, chemical interactions between the microcapsule's shell and core were also examined.

Morphology and Particle Study

To examine the surface morphology, distribution and aggregation, core shell structure of the microcapsule shell, Scanning Electron Microscopy (SEM) (SEM-FEI Quanta 200) and Polarized Optical Microscopy (POM) (POM-Olympus-BX41) were utilized. Additionally, Dynamic Light Scattering (DLS-Malvern) was used to analyse the Particle Size Distribution (PSD). This was achieved by dissolving the microcapsule in water and sonication for 20 min to determine the typical range of microcapsule sizes.

Thermogravimetric analysis (TGA) using the TGA-STA 7300-Hitachi instrument was conducted to determine the thermal degradation temperature of various samples, including SA-MA eutectic PCM, MF shell, plain microcapsules, and microcapsules containing GO, HDPE, and microcapsule-filled HDPE. The Lee method experiment, as shown in Fig. 2, was performed to determine the highest effective GO loading by assessing the thermal conductivity of microcapsules. For this test, a circular disc with a diameter of eleven centimetres was used as the sample, which was created by combining microcapsules ranging from 0% to 1.2% GO with HDPE at a 20% loading using a twin-screw extruder. The microcapsule loading in HDPE was kept constant while the GO loading was varied as the variable of interest. The resulting material was compression-moulded into a sheet shape, which was then cut into an 11 cm circular disc. The circular disc was placed between a solid plate and a steam cylinder, as shown in Fig. 2, and the system was suspended in the air with the aid of a platform. The temperature of the solid plate was denoted as T2, while the temperature of the steam cylinder was denoted as T1. The steam cylinder was removed once T2 stopped rising, and the remaining setup was left on a heating plate until T2 increased to T2 + 20, at which
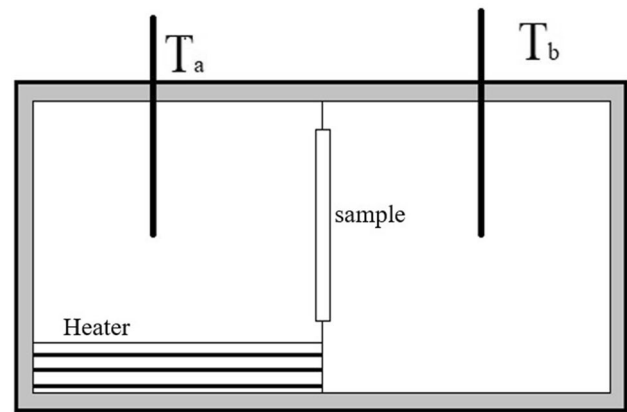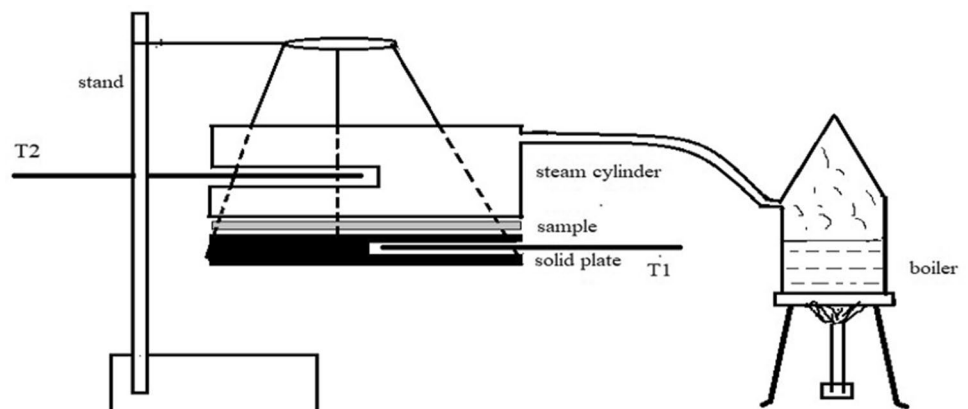

Fig. 3 Custom made heat transfer rate equipment

point the heating plate was removed, and T2 was noted as it decreased with respect to time until it reached T2-20.

$$K = \frac{m \times s \times slope \times thickness}{T2 - T1} \times area \tag{3}$$

where,

K = Thermal conductivity; m = mass = 1044 g; s = specific heat = 0.09.

Heat Transfer Rate

The heat transfers through the PCM microcapsule-filled HDPE composite was measured using a specially designed thermal energy transfer equipment. The equipment consists of two chambers between which the samples were placed, as shown in Fig. 3. The temperature in the second chamber was monitored over time, while the first chamber was heated at a regulated pace of 1 °C every 5 min.

Fig. 2 Set up for Lee's Method

Mechanical Properties

The mechanical properties of the HDPE composite filled with microcapsules were evaluated based on ASTM standards. Specifically, the tensile strength and impact resistance were tested using ASTM D 638 on a universal testing machine (UTM) with a load cell of 100 kg and an elongation limit of 50 mm/min. Additionally, the impact test was conducted using ASTM D 6110 on a Tinuis Olsen IT 504 pendulum impact tester, with a pendulum weight of 4.635 N and energy of 1.9676 J.

Results and Discussion

Thermal Properties

The DSC curves of the SA-MA PCM, MEPCM, GO-MEPCM, and GO-MEPCM-HDPE composite are depicted in Fig. 4. SA-MA PCM melts at 42.73 °C with a latent heat of melting of 145.1 J/g, and it crystallizes at 36.99 °C with a latent heat of crystallization of 139.4 J/g. Although the microcapsules and composite material exhibit similar phase behaviour as PCM, their heat enthalpies are lower. It is also noteworthy that the latent heat of MEPCM and GO-MEPCM is almost the same as that of the GO-MEPCM-HDPE composite material, indicating low loss of MEPCM during composite formation. Table 3 provides specific values.

The encapsulation method and material used in [24] shows the latent heat of material decrease as the GO content increases. However, the thermal conductivity increase observed in the MEPCM is in a similar range to that achieved in the composite material developed in this study.

Table 3 Thermal performance

| Sample	T_m (°C)	T_c (°C)	ΔH_m (J/g)	ΔH_c (J/g)
SA-MA PCM	42.73	36.99	145.1	139.4
MEPCM	41.06	35.03	76.88	72.52
GO-MEPCM	41.49	35.09	73.45	69.05
GO-MEPCM-HDPE	42.38	34.71	74.10	60.11

Thermal Stability

Figure 5 depicts the thermal stability of various materials including SA-MA PCM, MF-shell, MEPCM, GO-MEPCM, HDPE, MEPCM-HDPE, and GO-MEPCM-HDPE. It can be observed that the pure SA-MA PCM exhibits a single-step degradation, commencing from 200 °C. Similarly, the MF-shell material also undergoes a one-step degradation, starting at 385 °C and continuing until 420 °C, with a char yield percentage of 29.3%. On the other hand, MEPCM and GO-MEPCM exhibit a two-step degradation, with the first step occurring at the temperature range of SA-MA PCM, followed by the second step at the temperature range of MF-shell, indicating that the core degrades before the shell. Moreover, the weight loss rate of pure SA-MA PCM is higher compared to MEPCM, suggesting that the MF-shell enhances the thermal stability of SA-MA PCM. Furthermore, the composite sample also undergoes a two-stage degradation process, with the first stage associated with the microcapsule and the second stage associated with the HDPE component. Specific weight loss temperatures and char yields for each sample are provided in Table 4.
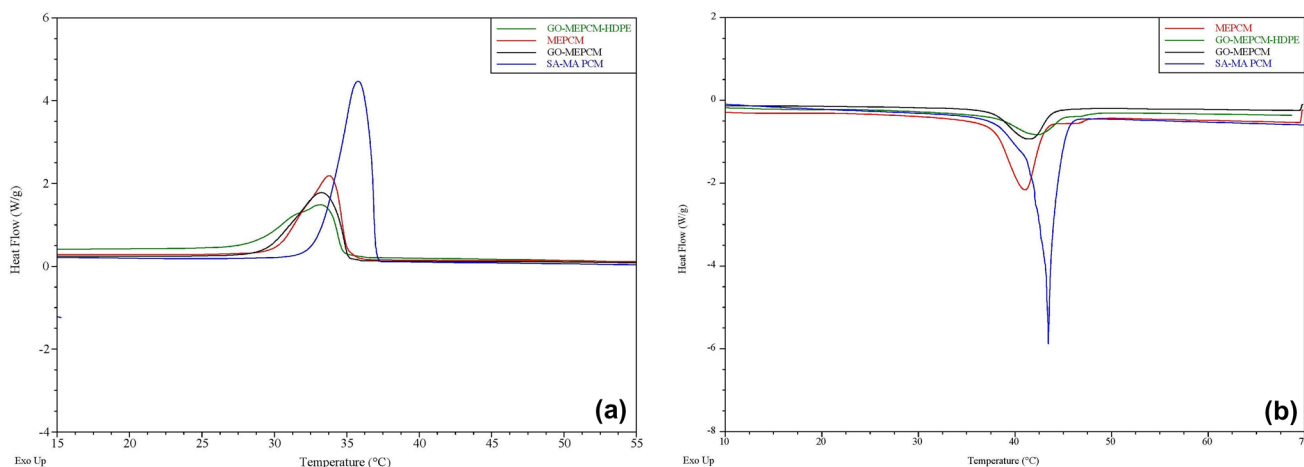
Fig. 4 DSC curve **a** Tc **b** Tm

**Fig. 5** Thermal stability of SA-MA PCM, MF-shell, MEPCM, GO-MEPCM, HDPE, GO-MEPCM-HDPE
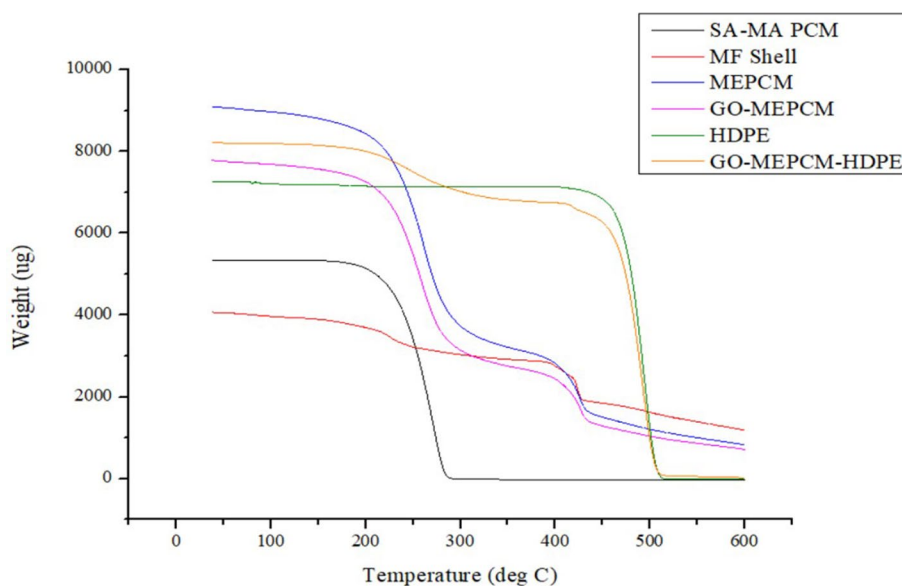
Table 4 Thermal stability data

Sample	First step degradation temperature (°C)		Second step degradation temperature (°C)		Char Yield %
	Start	End	Start	End	
SA-MA PCM	200	290	–	–	0.003
MF-Shell	385	420	–	–	29.3
MEPCM	210	300	395	440	9.14
GO-MEPCM	209	302	394	437	9.23
HDPE	415	515	–	–	3.20
GO-MEPCM–HDPE	210	320	420	515	3.17

Chemical Composition

The attenuated total reflectance (ATR) method was used to investigate the Fourier transform infrared spectroscopy (FTIR) spectra of GO, MEPCM, and GO/MEPCM, as illustrated in Fig. 6. Both types of microcapsules exhibit similar FTIR spectra, with stretching vibration peaks of the SA-MA spectrum at 2914.29 cm^{-1} and 2848.72 cm^{-1}, as well as the bending vibration peak of C-H, CH$_2$, and CH$_3$ at 1694.36 cm^{-1}, indicating the presence of SA-MA in the final product. Additionally, both types of microcapsules exhibit triazine ring vibration peaks at 1553.4 cm^{-1} of the MF poly-mer. The weak peak at 1100 cm^{-1} corresponds to C–O–C

Fig. 6 FTIR spectra of SA-MA, MF polymer, GO, MEPCM and GO/MEPCM
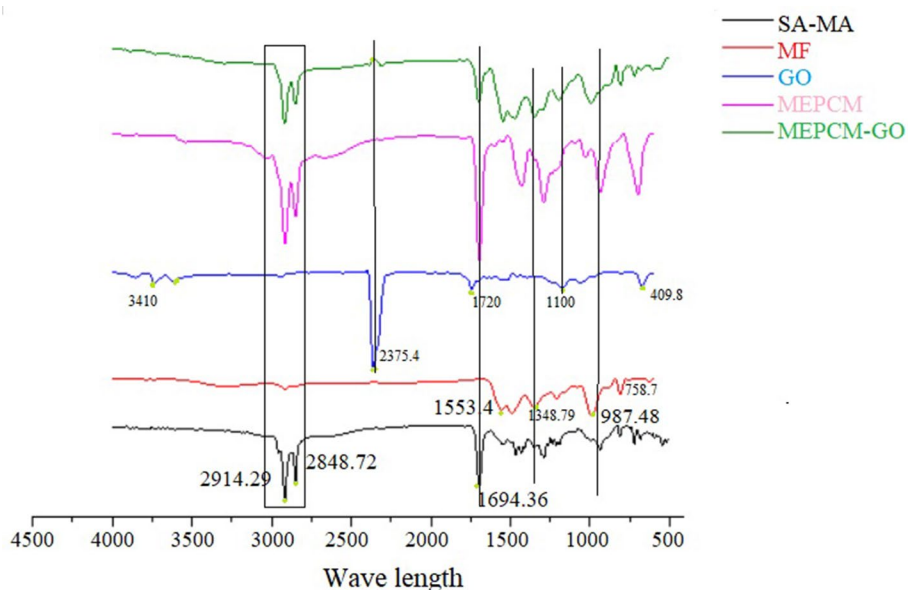
stretching vibration, and the peak at 987.4 cm^{-1} shows C-O stretching vibration of alcohol compounds, attributing to the existence of hydroxyl groups in the MF polymer. The existence of GO is confirmed by a small variation in the GO/MEPCM spectrum at 2375.4 cm^{-1}, as well as peaks at 1720 cm^{-1} and 1100 cm^{-1}. The small peak intensities in the GO spectra and GO/MEPCM may be related to GO's porosity. Peaks at 3410 cm^{-1} and 1100 cm^{-1} indicate that the GO has a -OH and C-O linkage. Comparison with the same chemical content of the shell material used in [24] and FTIR results in this study indicate similar peak range for MF polymer and GO, with similar overlaying spectra of MEPCM.

Morphology study of Microcapsule

The morphology of plain MEPCM and GO-MEPCM was investigated using scanning electron microscopy (SEM). As shown in Figs. 7a, b, the microcapsules in both cases appear to be nearly spherical. The size range of plain MEPCM is between 2–6 μm, while GO–MEPCM is slightly larger, with a size range of 2–12 μm. Figures 7c, d are enlarged versions of the same figure. It can be observed from Fig. 7c that GO-MEPCM has a rough structure, with small flakes adhering to the shell and collected flakes depicted by blue arrows. In contrast, plain MEPCM has a relatively smooth structure. Overall, this comparison suggests that GO is bonded to the shell, creating a slightly rough surface.

Upon examination using a polarised optical microscope, the PCM droplets display dark circular outer covers, as depicted in Fig. 8a and b. This observation suggests the presence of an amorphous polymeric shell (MF shell) that has formed, confirming the establishment of the core–shell structure. The POM micrographs align with the SEM photos, as the complete rounded engulfment can be observed.
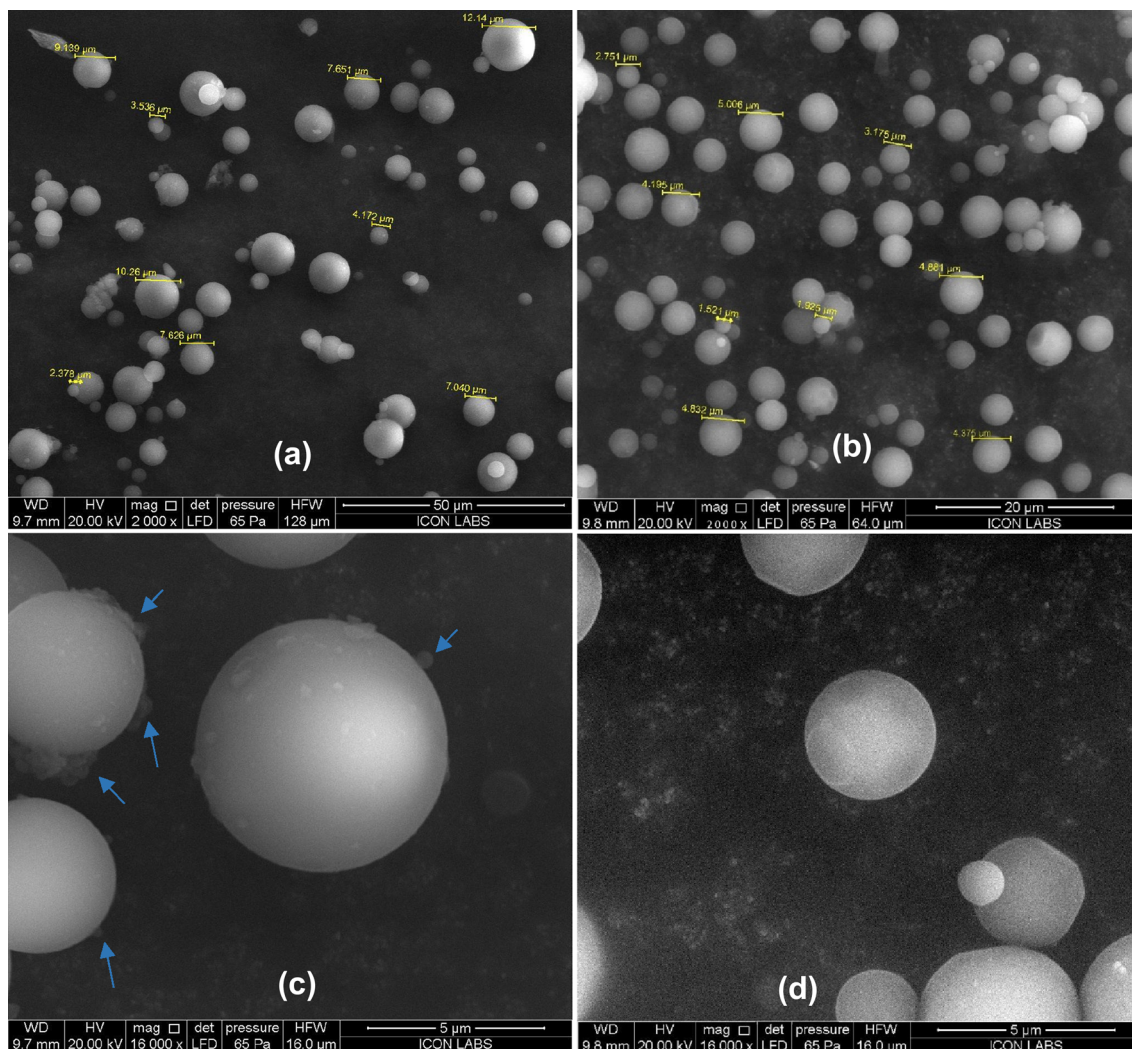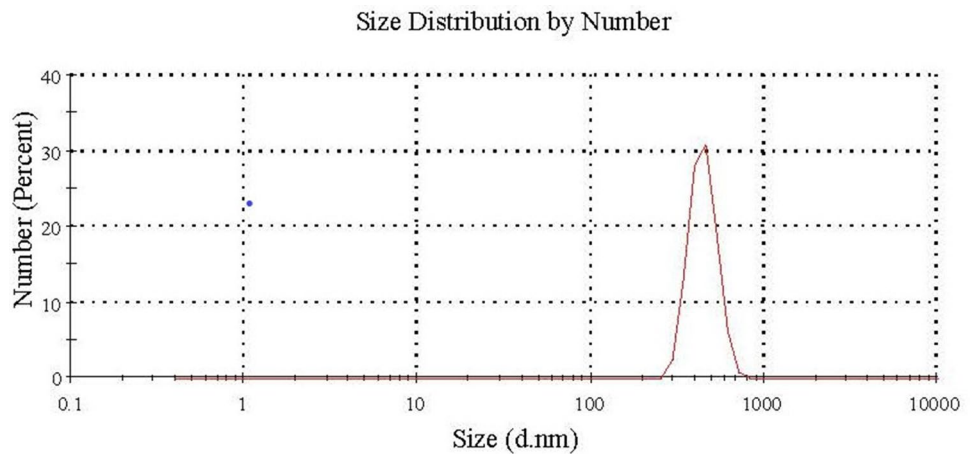

Fig. 7 SEM images **a** GO-MEPCM 2000X **b** Plain MEPCM 2000X **c** GO-MEPCM 16000X **d** Plain MEPCM 16000X
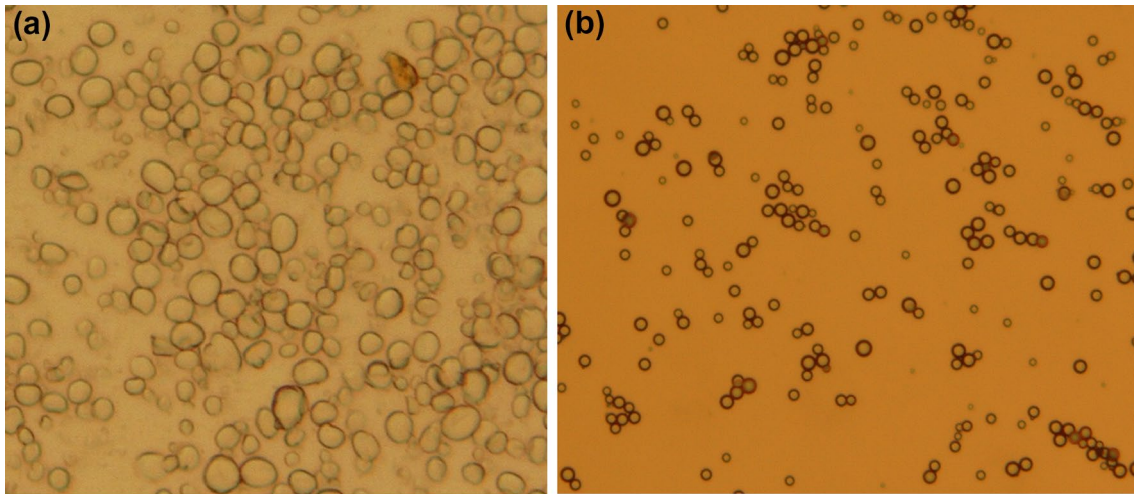
Fig. 8 images **a** POM micrograph of emulsion **b** POM micrograph of MEPCM

Fig. 9 Particle size distribution

The particle size distribution of the microcapsule with GO was analysed using DLS. As shown in Fig. 9, the distribution was found to be wide-ranging, with both nano and micro sized capsules present, although the majority fell between 0.1 μm and 1 μm. The Z-average diameter and polydispersity of the microcapsules were determined to be 719.9 nm and 0.503, respectively.

Thermal Conductivity

A small amount of graphene oxide (GO) can significantly improve the thermal conductivity of a material. Therefore, it is crucial to understand the GO quantity threshold value, as illustrated in Fig. 10. Below 1 wt.% of GO loading, thermal conductivity increases significantly, while increases after this point are small. The highest percentage increase of 47.5% is observed in the 0.8 wt.% GO MEPCM, which has a thermal conductivity of 0.575 W/m/K, as shown in

Table 5. This may be due to the fact that 0.8% of GO, with its 2D structure and high thermal conductivity, is sufficient to create a strong heat-transmitting channel within and outside the shell, allowing heat to pass through the shell with ease. In comparison to 0.8 wt.% GO, the increase in thermal conductivity is smaller in the 1 wt.% and 1.2 wt.% GO MEPCMs. In a study by [24] n-dodecanol is used as a PCM and encapsulated in a GO-modified MF shell, and the thermal conductivity results show the same trend. Thermal conductivity increases with an increase in GO content below 1 wt.%. The maximum rise achieved is 66.29% at 4 wt.% of GO, but the optimum value is 43.73% at 0.8 wt.% GO.

Heat Transfer Rate

To analyse the rate of heat transfer through the HDPE-MEPCM composite, a specially designed apparatus is used (refer to Fig. 3). In this experiment, a sample sheet is

Fig. 10 Thermal Conductivity vs. % GO Content
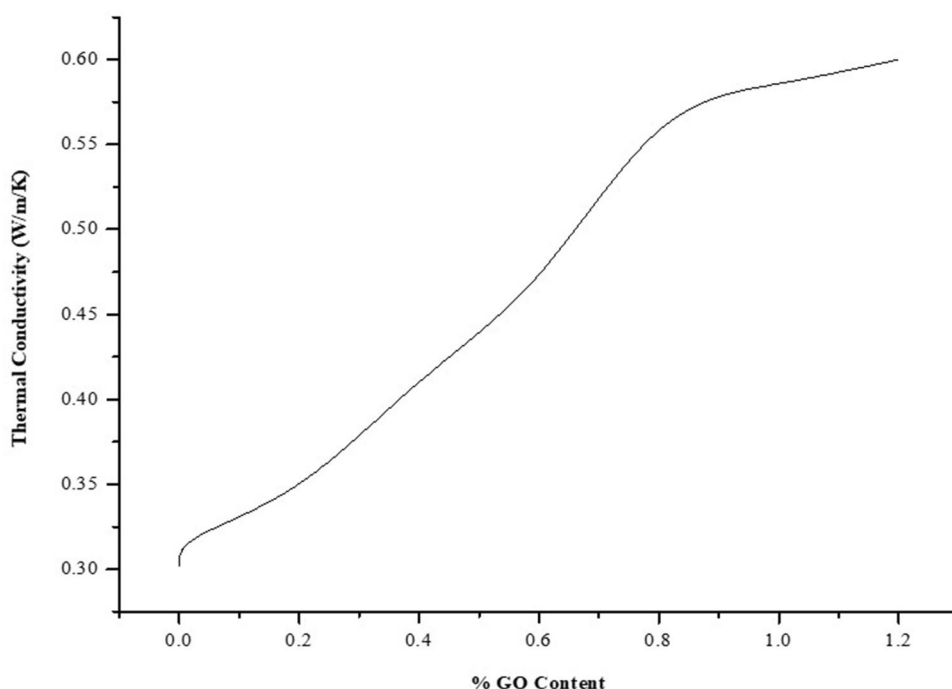
employed to separate chambers A and B. The time taken by chamber B to attain the predetermined temperature of chamber A is recorded. Chamber A is heated using heaters at the bottom at a specific rate of 1 °C/5 min. The temperature in chamber A is measured by Ta, and chamber B's temperature is indicated by Tb. The time required for virgin HDPE, plain 20, plain 30, plain 40, GO 20, GO 30, and GO 40 composites is depicted in graph (Fig. 11) as 135 ± 5 min, 155 ± 5 min, 185 ± 5 min, 205 ± 5 min, 170 ± 5 min, 190 ± 5 min, 230 ± 5 min. This indicates that the time required to attain a target temperature of 50 °C increases with an increase in the amount of MEPCM loading, and that composites incorporating GO require more time than equivalent plain composites. This delay may be due to the presence of GO, which provides greater heat transfer to the core and melts uniformly throughout, slowing down the temperature rise.

Table 5 Thermal Conductivity details indicating % increase

Material	Thermal conductivity (K, W/m/K)	%Increase
HDPE	0.301	0
Plain	0.3186	5.38
0.2 GO	0.342	11.98
0.4 GO	0.414	27.19
0.6 GO	0.462	34.84
0.8 GO	0.575	47.5
1 GO	0.584	48.4
1.2 GO	0.599	49.7

Therefore, GO 40 requires 95 more minutes than HDPE without MEPCM.

Mechanical Properties

The addition of microcapsules as a filler has dramatically reduced the tensile strength and impact strength of the material. This is because microcapsules function as stress concentration points. During a tensile test, when the high-density polyethylene (HDPE) is stretched, the microcapsules remain unchanged and create a point of stress that weakens the material, eventually leading to its fracture.

When the hammer strikes a sample during an impact test, the stress points created by the microcapsule can cause the sample to break. These stress points become more prominent as the microcapsule loading increases, which ultimately weakens the material. As a result, the strength values of microcapsules containing GO are significantly lower, as shown in both Fig. 12 and Fig. 13. The results of the tensile tests and Charpy impact tests for all variations of composite materials are provided in Tables 6 and 7.
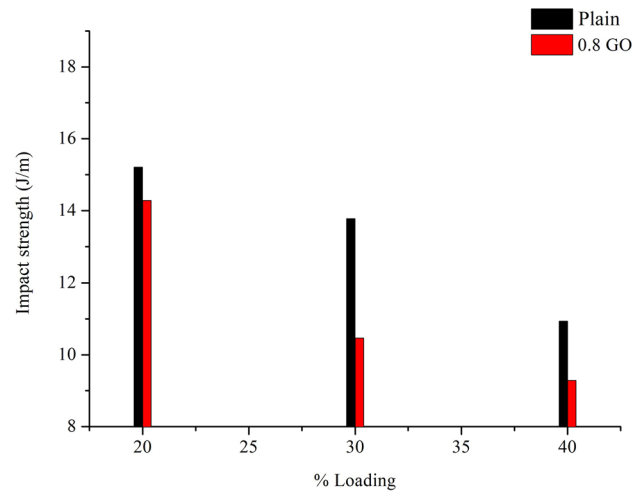
Conclusion

A single melting point of 42 °C was achieved for the eutectic mixture of stearic acid and myristic acid in the ratio of 6.71:73.14 wt.%. This eutectic mixture acted as a phase change material (PCM) in microcapsules that were prepared by an in-situ polymerization process with a g-MF shell. The

Fig. 11 Temperature vs Time graph
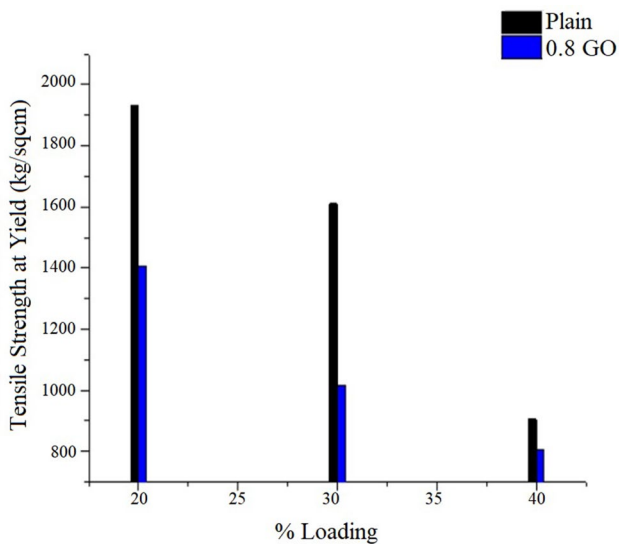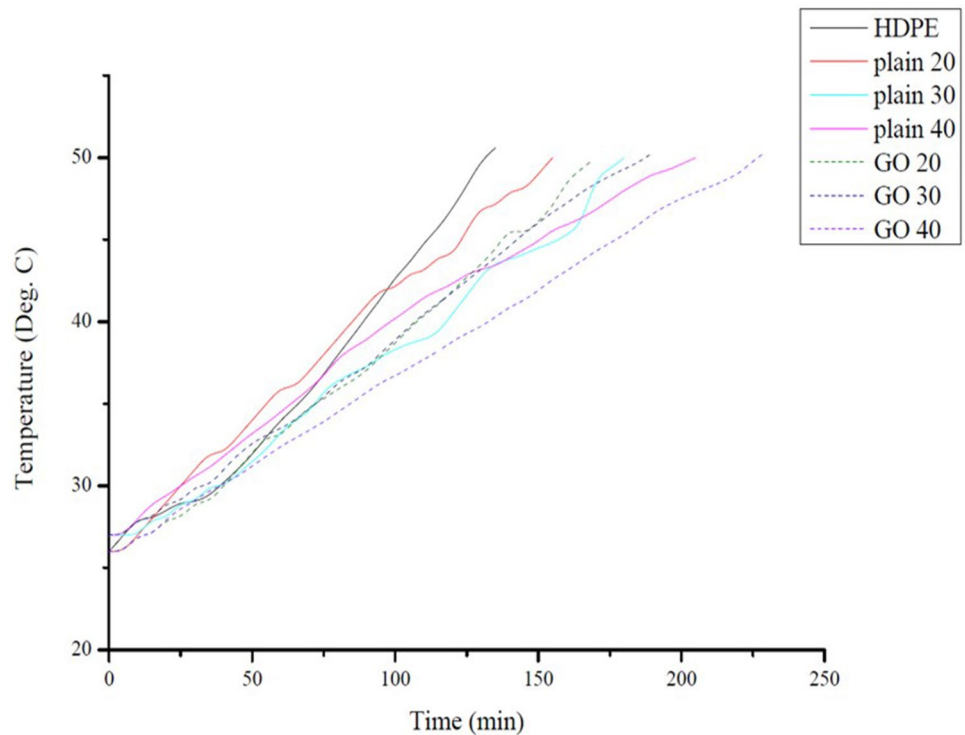
Fig. 12 % Loading vs Tensile strength at yield

Fig. 13 % Loading vs. Impact strength

success of the preparation was verified through a series of characterizations and tests, including FTIR, TGA, DSC, and SEM. The results of SEM, POM, and FTIR confirmed the formation of smooth core–shell structures, where the core did not interact with the shell or vice versa. The SEM images indicated that the addition of GO to the shell caused a slightly rougher surface morphology of the microcapsules compared to those with a plain MF shell. The TGA results demonstrated that microencapsulation improved the thermal

stability of the PCM to some extent. The results of this study were compared with those of previous studies [24] and [25] where the same shell material was used, but different methods of GO incorporation and encapsulation were employed, along with different PCMs. Wherever possible, a detailed comparison was made between the results obtained in this study and those in previous studies.

In composite materials, the microcapsule fillers function as point stresses, which can significantly reduce the mechanical properties of the composite. The results of

Table 6 Tensile Properties

Sample	Break Load (kg)	Yield Load (kg)	% Elongation at Break	% Elongation at Yield	Tensile strength at Break (kg/cm^2)	Tensile strength at Yield (kg/cm^2)	Ultimate modulus (MPa)
Virgin HDPE	47.6	73.2	43.45	11.28	1586.667	2440	8386.883
	41.3	66.9	43.1	11.03	1376.667	2230	4915.576
Plain 20	10	58	28.28	12.07	333.33	1933.333	4699.094
	9.6	54.4	15.83	110.3	320	1813.333	4915.977
Plain 30	31.2	48.3	22.21	14.8	1040	1610	3180.926
	6.7	46.8	29.3	13.66	223.333	1560	4915.976
Plain 40	27.2	27.2	4.66	4.66	906.667	906.667	2891.75
	23	23	4.9	4.9	766.667	766.667	2192.906
0.8 GO 20	36.7	37.4	8.52	7.38	1223.333	1246.667	4337.625
	41.5	42.2	8.76	7.96	1386.667	1406.626	4048.45
0.8 GO 30	30.2	30.5	6.61	6.15	1006.667	1016.667	4048.45
	27.5	27.7	4.99	4.76	916.667	923.333	3759.276
0.8 GO 40	24.1	24.1	3.75	3.75	803.333	803.333	4626.8
	19.8	19.8	2.7	2.7	660	660	4337.626

Table 7 Impact Strength (J/m)

Sample	No. of sample	Strength (J/m)	Average Strength
Virgin HDPE	1	38.577	32.980
	2	28.798	
	3	31.564	
Plain 20	1	20.081	15.121
	2	16.066	
	3	9.216	
Plain 30	1	13.951	13.775
	2	15.092	
	3	12.283	
Plain 40	1	7.237	10.938
	2	13.951	
	3	11.627	
0.8 GO 20	1	13.283	14.284
	2	16.574	
	3	12.996	
0.8 GO 30	1	10.006	10.466
	2	8.226	
	3	13.167	
0.8 GO 40	1	7.23	9.287
	2	11.48	
	3	9.152	

The aim of introducing GO into the MEPCM was to improve the thermal conductivity of the shell material. GO was added to increase the heat transfer rate through the shell since organic shell materials, like MF polymer, have low thermal conductivity. The addition of GO did not affect the melting point of the core material, as confirmed by the DSC results, which showed that the melting point remained nearly the same at 42°C. However, the composite material with GO-MEPCM had higher thermal conductivity (0.342–0.59 W/m/K) than the composite material with plain MEPCM (0.3186 W/m/K), as demonstrated by the thermal conductivity results. The heat transfer rate results also showed that the time required to reach the target temperature with plain MEPCM was lower than that required with GO-MEPCM, which suggests an improvement in thermal conductivity due to the presence of GO.

Declarations

Conflict of interest The authors declare that they have no known competing financial interests or personal relationships that could have appeared to influence the work reported in this paper.

the tensile and impact strength tests showed that the GO-MEPCM-HDPE composite had lower strength than the MEPCM-HDPE composite, which is consistent with similar trends seen in previous studies [37]

References

1. Mahlia TMI, Saktisahdan TJ, Jannifar A, Hasan MH, Matseelar HSC (2014) A review of available methods and development on energy storage; Technology update. Renew Sustain Energy Rev 33:532–545. https://doi.org/10.1016/j.rser.2014.01.068

2. Alva G, Liu L, Huang X, Fang G (2017) Thermal energy storage materials and systems for solar energy applications. Renew Sustain Energy Rev 68:693–706. https://doi.org/10.1016/j.rser.2016.10.021

3. Hasnain SM (1998) Review on sustainable thermal energy storage technologies, part 1: heat storage materials and techniques. Energy conversion and management 39(11):1127–1138

4. Sari A (2005) Eutectic mixtures of some fatty acids for low temperature solar heating applications: thermal properties and thermal reliability. Appl Therm Eng 25(14–15):2100–2107. https://doi.org/10.1016/j.applthermaleng.2005.01.010

5. Yuan Y, Zhang N, Tao W, Cao X, He Y (2014) Fatty acids as phase change materials: A review. Renew Sustain Energy Rev 29:482–498. https://doi.org/10.1016/j.rser.2013.08.107

6. Zhao P, Yue Q, He H, Gao B, Wang Y, Li Q (2014) Study on phase diagram of fatty acids mixtures to determine eutectic temperatures and the corresponding mixing proportions. Appl Energy 115:483–490. https://doi.org/10.1016/j.apenergy.2013.10.048

7. Sari A, Kaygusuz K (2006) Thermal energy storage characteristics of myristic and stearic acids eutectic mixture for low temperature heating applications. Chinese J Chem Eng 14(2):270–275. https://doi.org/10.1016/S1004-9541(06)60070-0

8. Nazir H, Batool M, Ali M, Kannan AM (2018) Fatty acids based eutectic phase change system for thermal energy storage applications. Appl Therm Eng 142:466–475. https://doi.org/10.1016/j.applthermaleng.2018.07.025

9. Wei H, Xie X, Li X, Lin X (2016) Preparation and characterization of capric-myristic-stearic acid eutectic mixture/modified expanded vermiculite composite as a form-stable phase change material. Appl Energy 178:616–623. https://doi.org/10.1016/j.apenergy.2016.06.109

10. Yanping Y, Wenquan T, Xiaoling C, Li B (2011) Theoretic prediction of melting temperature and latent heat for a fatty acid eutectic mixture. J Chem Eng Data 56(6):2889–2891

11. Zhang N, Yuan Y, Du Y, Cao X, Yuan Y (2014) "Preparation and properties of palmitic-stearic acid eutectic mixture / expanded graphite composite as phase change material for energy storage. Energy. https://doi.org/10.1016/j.energy.2014.10.092

12. Guo X, Cao J, Peng Y, Liu R (2016) Incorporation of microencapsulated dodecanol into wood flour / high-density polyethylene composite as a phase change material for thermal energy storage. JMADE 89:1325–1334. https://doi.org/10.1016/j.matdes.2015.10.068

13. Cai Y, Wei Q, Huang F, Lin S, Chen F, Gao W (2009) "Thermal stability, latent heat and flame retardant properties of the thermal energy storage phase change materials based on paraffin / high density polyethylene composites. Renew Energy 34:2117–2123. https://doi.org/10.1016/j.renene.2009.01.017

14. Hassabo AG, Mohamed AL, Wang H, Popescu C, Moller M (2015) Metal salts rented in silica microcapsules as inorganic phase change materials for textile usage. Inorganic Chemistry: An Indian Journal 10(2):59–65

15. Mahamad Dom AB, Tulos NA, Wan Ahmad WY, Mohd AF, Yahya MF (2016) Thermal conductivity of paraffin wax as microencapsulated phase change material (PCM) coated on polyester fabric. Adv Mater Res 1134:160–4. https://doi.org/10.4028/www.scientific.net/AMR.1134.160

16. Sari A, Alkan C, Karaipekli A, Uzun O (2009) Microencapsulated n- octacosane as phase change material for thermal energy storage. Sol Energy 83(10):1757–1763. https://doi.org/10.1016/j.solener.2009.05.008

17. Srinivasaraonaik B, Singh LP, Tyagi I, Rawat A, Sinha S (2020) Microencapsulation of a eutectic PCM using in situ polymerization technique for thermal energy storage. Int J Energy Res 8:1–11. https://doi.org/10.1002/er.5182

18. Bao Y, Pan W, Wang T, Wang Z, Wei F, Xiao F (2011) Microencapsulation of fatty acid as phase change material for latent heat storage. J Energy Eng. https://doi.org/10.1061/(ASCE)EY.1943-7897.0000053

19. Xin ZH, Wei Y (2015) Preparation of urea-formaldehyde paraffin microcapsules modified by carboxymethyl cellulose as a potential phase change material. J For Res. https://doi.org/10.1007/s11676-015-0027-y

20. Liu W, Zhang X, Ji J, Wu Y, Liu L (2021) A review on thermal properties improvement of phase change materials and its combination with solar thermal energy storage. Energy Technol. https://doi.org/10.1002/ente.202100169

21. Xu C, Zhang H, Fang G (2022) Review on thermal conductivity improvement of phase change materials with enhanced additives for thermal energy storage. J Energy Storage. https://doi.org/10.1016/j.est.2022.104568

22. Lin Y, Jia Y, Alva G, Fang G (2017) Review on thermal conductivity enhancement, thermal properties and applications of phase change materials in thermal energy storage. Renew Sustain Energy Rev. https://doi.org/10.1016/j.rser.2017.10.002

23. Zhao Q, He F, Zhang Q, Fan J, He R, Zhang K, Yan H, Yang W (2019) Microencapsulated phase change materials based on graphene Pickering emulsion for light-to-thermal energy conversion and management. Sol Energy Mater Sol Cells. https://doi.org/10.1016/j.solmat.2019.110204

24. Chen Z, Wang J, Yu F, Gao X (2015) Preparation and properties of graphene oxide- modified poly(melamine-formaldehyde) microcapsules containing phase change material n- dodecanol for thermal energy storage. Urnal marials Chem A 5:11624–11630. https://doi.org/10.1039/C5TA01852H

25. Zhao Q, Yang W, Li Y, He Z, Li Y, Zhou Y, Wang R, Fan J, Zhang K (2020) Multifunctional phase change microcapsules based on graphene oxide Pickering emulsion for photothermal energy conversion and superhydrophobicity. Int J Energy Res 44:4464–4474. https://doi.org/10.1002/er.5224

26. Liu Z, Chen Z, Yu F (2019) Enhanced thermal conductivity of microencapsulated phase change materials based on graphene oxide and carbon nanotube hybrid filler. Sol Energy Mater Sol Cells 192:72–80. https://doi.org/10.1016/j.solmat.2018.12.014

27. Maithya OM, Li X, Feng X, Sui X (2020) Microencapsulated phase change material via Pickering emulsion stabilized by graphene oxide for photothermal conversion. J Mater Sci 55(18):7731–7742. https://doi.org/10.1007/s10853-020-04499-5

28. Peng G, Dou G, Hu Y, Sun Y, Chen Z (2020) Phase change material (PCM) microcapsules for thermal energy storage. Hindawi Adv Polym Technol 9:6–7. https://doi.org/10.1155/2020/9490873

29. Prajapati DG, Kandasubramanian B (2020) A Review on polymeric-based phase change material for thermo-regulating fabric application. Polym Rev 60(3):389–419. https://doi.org/10.1080/15583724.2019.1677709

30. Alva G, Lin Y, Liu L, Fang G (2017) Synthesis, characterization and applications of microencapsulated phase change materials in thermal energy storage: a review. Energy Build 144:276–294. https://doi.org/10.1016/j.enbuild.2017.03.063

31. Mohaddes F, Islam S, Shanks R, Fergusson M, Wang L, Padhye R (2014) Modification and evaluation of thermal properties of melamine- formaldehyde / n-eicosane microcapsules for

thermo-regulation applications. Appl Therm Eng 71(1):11–15. https://doi.org/10.1016/j.applthermaleng.2014.06.016

32. Chen Z, Fang G (2011) Preparation and heat transfer characteristics of microencapsulated phase change material slurry : a review. Renew Sust Energy Rev 15:4624–4632. https://doi.org/10.1016/j.rser.2011.07.090

33. Jeong S-G, Chang SJ, Wi S, Kang Y, Kim S (2015) Development and performance evaluation of heat storage paint with MPCM for applying roof materials as basic research. Energy Build. https://doi.org/10.1016/j.enbuild.2015.12.001

34. Cai Y, Wei Q, Huang F, Gao W (2008) Preparation and properties studies of halogen-free flame retardant form-stable phase change materials based on paraffin / high density polyethylene composites. Appl Energy 85:765–775. https://doi.org/10.1016/j.apenergy.2007.10.017

35. Karkri M, Lachheb M, Nogellova Z, Boh B, Sumiga B, Almaadeed MA, Fethi A, Kurpa I (2014) Thermal properties of phase-change materials based on high-density polyethylene filled with microencapsulated paraffin wax for thermal energy storage. Energy Build. https://doi.org/10.1016/j.enbuild.2014.11.061

36. Kurpa I, Nogellova Z, Spitalsky Z, Janigová I, Boh B, Sumiga B, Kleinova A, Kakri M, Almadeed MA (2014) Phase change materials based on high-density polyethylene filled with microencapsulated paraffin wax. Energy Convers Manag 87:400–409. https://doi.org/10.1016/j.enconman.2014.06.061

37. Valizadeh S, Ehsani M, Angji MT (2019) "Development and thermal performance of wood- HPDE- PCM nanocapsule floor for passive cooling in building. Energy Sources Part A: Recover Util Environ Eff 00(00):1–14. https://doi.org/10.1080/15567036.2018.1550125

38. Lv Y, Yang X, Li X, Zhang G, Wang Z, Yang C (2016) Experimental study on a novel battery thermal management technology based on low density polyethylene-enhanced composite phase change materials coupled with low fins. Appl Energy 178:376–382. https://doi.org/10.1016/j.apenergy.2016.06.058

39. Fredi G, Brunig H, Vogel R, Scheffler C (2019) Melt-spun polypropylene filaments containing paraffin microcapsules for multifunctional hybrid yarns and smart thermoregulating thermoplastic composites. Express Polym Lett. https://doi.org/10.3144/expresspolymlett.2019.93

40. Trigui A, Karkri M, Krupa I (2014) Thermal conductivity and latent heat thermal energy storage properties of LDPE / wax as a shape-stabilized composite phase change material. Energy Convers Manag 77:586–596. https://doi.org/10.1016/j.enconman.2013.09.034

41. Sari A (2004) Form-stable paraffin / high density polyethylene composites as solid – liquid phase change material for thermal energy storage : preparation and thermal properties. Energy Convers Manag 45:2033–2042. https://doi.org/10.1016/j.enconman.2003.10.022

42. Cai Y, Hu Y, Song L, Lu H, Chen Z, Fan W (2006) Preparation and characterizations of HDPE – EVA alloy / OMT nanocomposites / paraffin compounds as a shape stabilized phase change thermal energy storage material. Thermochimica Acta 451:44–51. https://doi.org/10.1016/j.tca.2006.08.015